

Novel Layer-by-Layer Procedure for Making Nylon-6 Nanofiber Reinforced High Strength, Tough, and Transparent Thermoplastic Polyurethane Composites

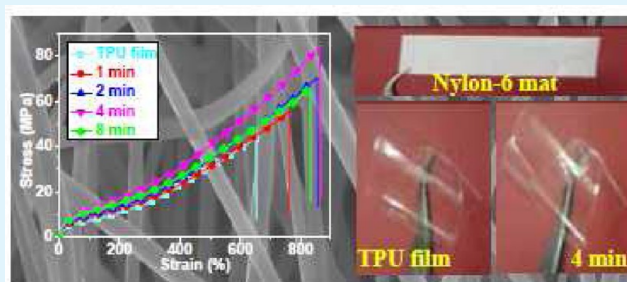
Shaohua Jiang,[†] Gaigai Duan,[†] Haoqing Hou,[‡] Andreas Greiner,[†] and Seema Agarwal^{*,†}

[†]Philipps-Universität Marburg, Department of Chemistry and Scientific Center of Materials Science, Hans-Meerwein-Str., D-35032 Marburg, Germany

[‡]Jiangxi Nanofiber Engineering Center, Jiangxi Normal University, Nanchang 330022, China

ABSTRACT: We highlight a novel composite fabrication method based on solution casting, electrospinning, and film stacking for preparing highly transparent nylon-6 nanofiber reinforced thermoplastic polyurethane (TPU) composite films. The procedure is simple and can be extended to the other thermoplastics. The morphology of fiber/matrix interface and the properties of composite films were also investigated. The method led to a significant reinforcement in mechanical properties of TPU like tensile strength, E modulus, strain, and toughness just using very small amounts of nylon fibers (about 0.4–1.7 wt %; 150–300 nm diameter). The enhanced mechanical properties were achieved without sacrificing optical properties like transparency of TPU.

KEYWORDS: electrospinning, nanocomposites, mechanical properties, transparency, nanofibers



1. INTRODUCTION

Thermoplastic polyurethanes (TPUs) are a special class of polymers widely used in different industries for varied applications like textile, footwear industry, tubings, biomaterials, and adhesives, to name a few.^{1–6} TPUs with different material property profiles are required for these applications and can easily be made by changing the chemical structure of the starting materials like diisocyanate, polyol, and the chain extender.⁷ Another easy and cost-effective method of changing properties of TPUs is using reinforcement fillers. Nanoparticles (nanoclay particles, silica nanoparticles)^{8,9} and fibers (aramid fibers, carbon fibers, glass fibers, etc.)^{10–12} have been used in the literature for improving the mechanical properties of TPUs.

In general, the key issues for producing high performance fiber reinforced polymer composites are the use of high strength fibers, large length/diameter ratio of fibers, good wetting procedure of fibers by matrix solution, homogeneous dispersion of fibers in matrix, and strong interfacial interaction between fibers and matrix. Polymer nanofibers produced by electrospinning have been attracting more and more attention for the preparation of composites. The continuous long fibers produced by electrospinning lack fiber edges (ends) and therefore do not have stress concentration points in composites. During the electrospinning, the polymer molecular chains tend to align along the fiber axis as the polymer jet is drawn up to 100 000 times in less than 0.1 s.¹³ These highly molecular oriented nanofibers can provide a mechanically strong fiber for the preparation of fiber reinforced composites. Also, electrospun nanofiber mats have high porosity and large

specific surface area. Therefore, nanofibers produced by electrospinning could be highly promising candidates for reinforcement purposes. Moreover, the diameters of electrospun nanofibers are usually less than the wavelength of visible light and expected to give transparent composites.^{14–16}

Despite so many advantages of nanofibers, only countable studies are available in the literature regarding the electrospun nanofiber reinforced composites. A recent review article¹⁷ is a good reference supporting this fact. Early reports of reinforcing effects of nanofibers in an epoxy and a rubber matrix (styrene-butadiene rubber) were contributed by Kim et al.¹⁸ They showed an increase in Young's modulus, fracture toughness, and fracture energy of the epoxy matrix. Bergshoef et al. showed the formation of transparent epoxy composites using 4 wt % nylon-4, 6 electrospun nanofibers (30–200 nm in diameter).¹⁴ Nylon-6 nanofibers produced by electrospinning exhibit excellent mechanical properties, such as toughness and high tensile strength,^{19,20} and have also been adopted to make composites with poly (methyl methacrylate),²¹ polyaniline,²² and polycaprolactone²³ and with bis-glycidyl methacrylate/tetraglycidylmethacrylate (BIS-GMA/TEGDMA) as dental restorative composites.^{24,25} Subsequently, cellulose,²⁶ polyvinyl alcohol (PVA),²⁷ polyacrylonitrile (PAN),^{28,29} polyimide,³⁰ and nylon-66³¹ nanofibers were reported to make nanofiber reinforced composites.

Received: June 6, 2012

Accepted: July 16, 2012

Published: July 20, 2012

Recently, we highlighted the importance of the nanofiber wetting procedure for the preparation of highly tough and transparent composites using nylon-6 as reinforcing fibers for Melamine formaldehyde.³² A change of the wetting method could bring about a drastic change in the morphology of the wet fibers. The wetting of nylon fibers by passing through a solution of MF resin showed a core-shell morphology and a significant improvement in properties as compared to the dip-coating procedure for wetting of the fibers. Different composites with varied amounts of nylon-6 fibers generated a profile of properties.

There are several conventional ways to fabricate fiber reinforced composites such as solution mixing and casting, melt mixing, and wetting of fibers by polymer matrix and subsequent stacking by hot-press. The method chosen should show uniform distribution and good wetting of the reinforcing material. In the present study, we highlight a novel composite fabrication method based on solution casting, electrospinning, and film stacking for preparing highly transparent nylon-6 nanofiber reinforced thermoplastic polyurethane composite films. The effect of this novel and quick wetting procedure on the morphology of fiber/matrix interface and on the properties of composite films were investigated using scanning electronic microscopy (SEM), attenuated total reflectance spectroscopy (ATR-IR), thermo gravimetric analysis (TGA), tensile testing, and UV-vis spectroscopy. A very small amount of nylon fibers could enhance the mechanical properties significantly without sacrificing optical properties like transparency of TPU. The results are presented here.

2. EXPERIMENTAL SECTION

2.1. Materials. Nylon-6 (Ultrad B24 NSD05, pellet size: 2.0–2.0 mm) was kindly supplied by BASF while thermoplastic polyurethane (TPU, Desmopan DP 2590A) was purchased from Bayer Materials Science. The solvents, formic acid (FA, ≥98%), acetic acid (AcOH, ≥98%), and anhydrous dimethyl formamide (DMF, 99.8%), were acquired from Sigma-Aldrich. All materials were used as received without further purification.

2.2. Electrospinning and Composite Fabrication. The fabrication of nylon-6 nanofiber reinforced TPU composites consists of solution casting, electrospinning, and film stacking. TPU (2.5 wt %) solution in DMF and 20 wt % nylon-6 solution in FA/AcOH (40/60, w/w) were used for film casting and electrospinning, respectively. The detailed composite preparation process is shown in Figure 1. It contains the following steps: (1) 1 mL of 2.5 wt % TPU solution in DMF was casted on a glass slide; (2) electrospinning of one thin layer of nylon-6 nanofibers on the wet TPU solution; (3) drying at 100 °C to obtain composite with one layer of TPU film and one layer of nylon-6 nanofibers; (4) repeat the above 3 steps (casting TPU solution, electrospinning nylon-6 nanofibers, and drying) for another 3 times; (5) casting the last layer of TPU solution and drying to gain a laminated composite with alternate layers of TPU and nylon-6 nanofibers (in total 3 layers of nylon-6 nanofibers sandwiched by 4 layers of TPU films). During the electrospinning, a 20 kV electrical potential was applied on the flat tip of the needle (diameter of 0.8 mm) while the distance between the needle tip and the glass slide was 20 cm.

Many different composites were made by keeping the amount of TPU constant but varying the amount of nylon-6 reinforcing fibers. The amount of nylon-6 fibers in composites was varied by carrying out electrospinning for different intervals of time, i.e., each layer of nylon-6 was spun for 1, 2, 4, or 8 min. The concentration of nylon-6 solution used for electrospinning was kept constant. The content of nylon-6 nanofibers in the composites was measured by gravimetry. All the composites had 4 layers of TPU (1 mL, 2.5 wt % in DMF) and 3 layers of nylon-6 nanofibers (each layer was electrospun for 1, 2, 4, or 8

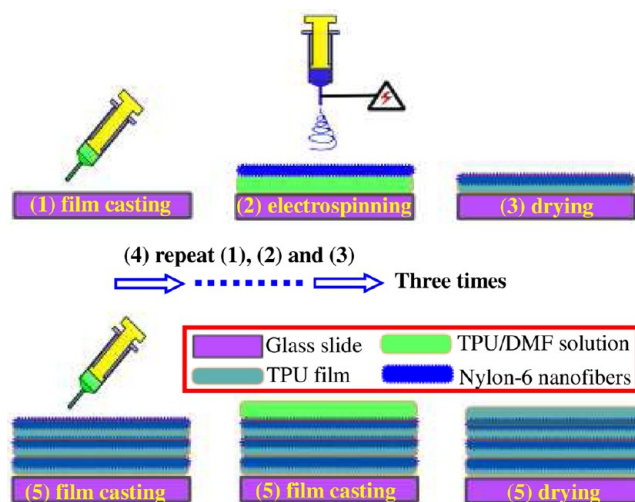


Figure 1. Schematic of the preparation of nylon-6 nanofiber reinforced TPU composite films.

min). The content of nylon-6 by weight ($C_{\text{nylon-6}}$) was calculated by the following equation:

$$C_{\text{nylon-6}} = \frac{3 \times m_{\text{nylon-6}}}{4 \times m_{\text{TPU}} + 3 \times m_{\text{nylon-6}}} \times 100\%$$

where m_{TPU} and $m_{\text{nylon-6}}$ stand for the weight of 1 layer of TPU and nylon-6 nanofibers, respectively. The electrospinning time of 1, 2, 4, and 8 min for each layer corresponded to 0.4, 0.9, 1.7, and 3.4 wt % of nylon-6 nanofibers in the laminated composites (4 layers of TPU films and 3 layers of nylon-6 nanofibers). As blanks, neat TPU films were made by casting 4 mL of (2.5 wt %) TPU/DMF solution, and nonwoven nylon-6 nanofiber mat was made by electrospinning 20 wt % nylon-6 in FA/AcOH (40/60, w/w).

2.3. Characterizations. The G10 contact angle analysis system (Kreuss, Hamburg, Germany) was used to test the wetting of the nylon-6 nanofiber mat with DMF. The surface morphology and the cross-section morphology of the TPU/nylon-6 nanofiber composites were observed by the JSM-7500 scanning electronic microscopy (SEM). Prior to scanning, the specimens were sputter-coated with gold for 120 s to avoid charge accumulations. Cross-section samples were prepared by breaking the frozen films in liquid nitrogen. Image J software was used to measure the diameter of nylon-6 nanofibers and to make a diameter distribution. ATR-IR spectra were recorded on a Digilab Excalibur Series with an ATR unit MIRacle from the company Pike Technology. The Zwick/Roell BT1-FR 0.5TN-D14 machine, equipped with a 200 N KAF-TC load sensor using a stretching rate of 50 mm/min, was applied to measure the mechanical properties. All the specimens were cut into dog-bone-shape with an average length of 3.0 cm and a central width of 0.2 cm. The Perkin-Elmer Lambda 9 UV-vis/NIR spectrophotometer operating in transmittance mode (200–800 nm) was used to characterize the optical properties. The Mettler Toledo TGA/SDTA 851e was carried to study the thermal properties at a heating rate of 10 °C/min in N_2 from 50 to 800 °C.

3. RESULTS AND DISCUSSION

3.1. Fabrication of TPU/Nylon-6 Nanofiber Composites. The long continuous nylon-6 nanofibers were fabricated by the process of electrospinning in this study. The resulted nylon-6 nanofibers were collected as nonwoven mat and had a smooth surface morphology as seen in Figure 2A. No defects such as beads, pores, or ribbons were found in/on the nanofibers. The ultrafine nylon-6 nanofibers displayed a centralized diameter distribution ranging from 150 to 300 nm (Figure 2B).

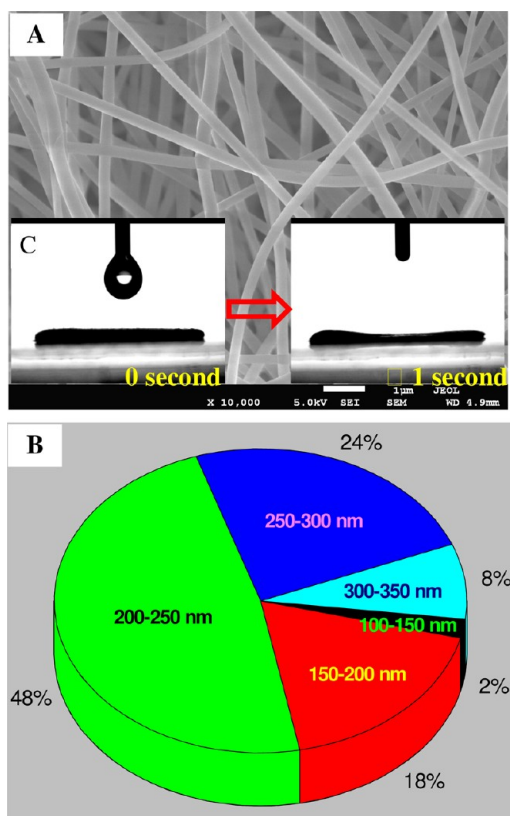


Figure 2. SEM image (A), pie chart of the diameter distribution (B), and DMF wetting behavior (C) of nylon-6 nanofiber mat. Scale bar of (A) = 1 μm .

For the fiber reinforced composites, it is important to embed the fibers into the polymer matrix. This in turn depends on the dispersion of fibers and good wetting between fibers and matrix. In one experiment, the nylon-6 nanofibers were collected on the dried TPU film. Because of the multilayered morphology of nanofiber mat and the cylinder/ellipsoid structure of nanofibers, only a part of the fibers was in contact with the TPU film (Figure 3A). This kind of nanofiber/matrix morphology (Figure 3A) provides a poor interfacial interaction between fibers and matrix, which would not be useful to fabricate high quality composites.

To achieve good wetting and embedding of reinforcing nylon-6 fibers in TPU matrix, the nylon-6 nanofibers were directly electrospun on the TPU/DMF solution in a layer-by-layer process. This procedure was adopted because of ultrafast wetting of nylon-6 nanofibers by DMF. Nylon-6 is not soluble in DMF but undergoes very fast wetting (in less than 1 s; Figure 2C). Therefore, the randomly deposited nanofibers on TPU/DMF solution ensured nice dispersion and homogeneous wetting of reinforcing nylon-6 nanofibers with TPU matrix. The nanofibers could be completely wetted quickly by the DMF solvent, subsequently sunk into the TPU resin while maintaining the morphology and formed tight contact with the resin (Figure 3B). Further, different experiments were carried out with varied amounts of nylon-6 nanofibers in the first layer. The amount of nanofibers was regulated by the time of electrospinning as described in the experimental part. The wetting behavior of nylon-6 nanofibers by DMF made the fibers completely embedded in the TPU matrix for low amounts of nylon fibers, i.e., electrospinning until about 4 min (Figure 3B,C); the increased thickness of the nanofiber layer with

increased spinning time (8 min) led to wetting of underneath layers, but top layers could not be impregnated completely (Figure 3D). Therefore, the layer-by-layer process of wetting reinforcing nylon fibers was used and another layer of TPU/DMF solution was casted on the surface of the 2-layered composites described above followed by electrospinning of nylon-6 again for the same time intervals, i.e., 1, 2, 4, and 8 min on different samples. The procedure was continued to make a TPU/nylon-6 composite film with 4 TPU layers sandwiching 3 layers of randomly oriented nylon fibers.

The resulted composite films revealed a smooth surface as shown in Figure 4B and had almost the same morphology as the neat TPU film (Figure 4A). The absence of nylon-6 nanofibers both on the surface of TPU/nylon-6 nanofiber composite film and on edges as pulled-out structures suggested a good dispersion of nanofibers in the TPU matrix.

The uniform dispersion of reinforcing nylon fibers could also be proved by the ATR-IR spectroscopy. There was no difference observed in spectra of neat TPU (Figure 5A), 2 layer composite film with ATR measured on TPU side (Figure 5G) and multilayered composite film (Figure 5H) with both sides (top and bottom) TPU layers. This confirmed the homogeneous distribution of fibers in bulk and no fibers on the surface. The ATR-IR was also recorded on 2-layer composite samples with the incident light directed from nylon-6 nanofiber side to TPU side (Figure 5B,C,D,E). The intensity of the characteristic peak of nylon-6 (carbonyl stretching, indicated with black arrow) increased from spectra (C) to (E) showing increased amount of the nylon-6 nanofiber in the 2 layered composites. Further, the carbonyl peak of nylon-6 in composites had a small red shift (1643 cm^{-1} for (C), (D), and (E); 1639 cm^{-1} for pure nylon-6 mat), which might be the result of hydrogen bonding between nylon-6 and TPU. Spectrum (B) did not show any characteristic peaks of nylon-6, and the ATR-IR spectrum was nearly the same as that of neat TPU (Figure 5A). This is due to the deposition of an extremely thin layer of nylon-6 nanofibers (electrospinning time of 1 min) in TPU, and all the nanofibers were embedded into the TPU matrix.

TPU and nylon-6 nanofiber mat showed a good resistance to heat. A 5% weight loss as determined by thermogravimetric analysis (TGA) was observed at 316 and 390 $^{\circ}\text{C}$ for TPU and nylon-6 nanofiber mat, respectively (TGA thermogram not shown here). After incorporating nylon-6 nanofibers into TPU matrix, the composites presented almost similar thermal behavior as that of neat TPU.

3.2. Mechanical Properties. Figure 6 shows the typical stress–strain curves of neat TPU film and TPU/nylon-6 nanofiber composite films. The average tensile properties such as tensile strength, elongation at break, and E modulus are summarized in Table 1. It can be seen that the neat TPU film revealed an average tensile strength of 42 MPa, E modulus of 27 MPa, and elongation at break of 673%. The TPU/nylon-6 nanofiber composite films displayed significantly high mechanical properties with even very small amounts of nylon fibers. The tensile strength and E modulus increased with an increase in the amount of reinforcing nylon-6 nanofibers until about 1.7 wt %. The tensile strength and E modulus were almost doubled with 1.7 wt % of reinforcing fibers with a significant increase in elongation at break. Although, further increase in the amount of nylon fibers to 3.4 wt % led to a drop in mechanical properties, but still, the mechanical properties were significantly higher than the neat TPU film. A similar trend was also observed for

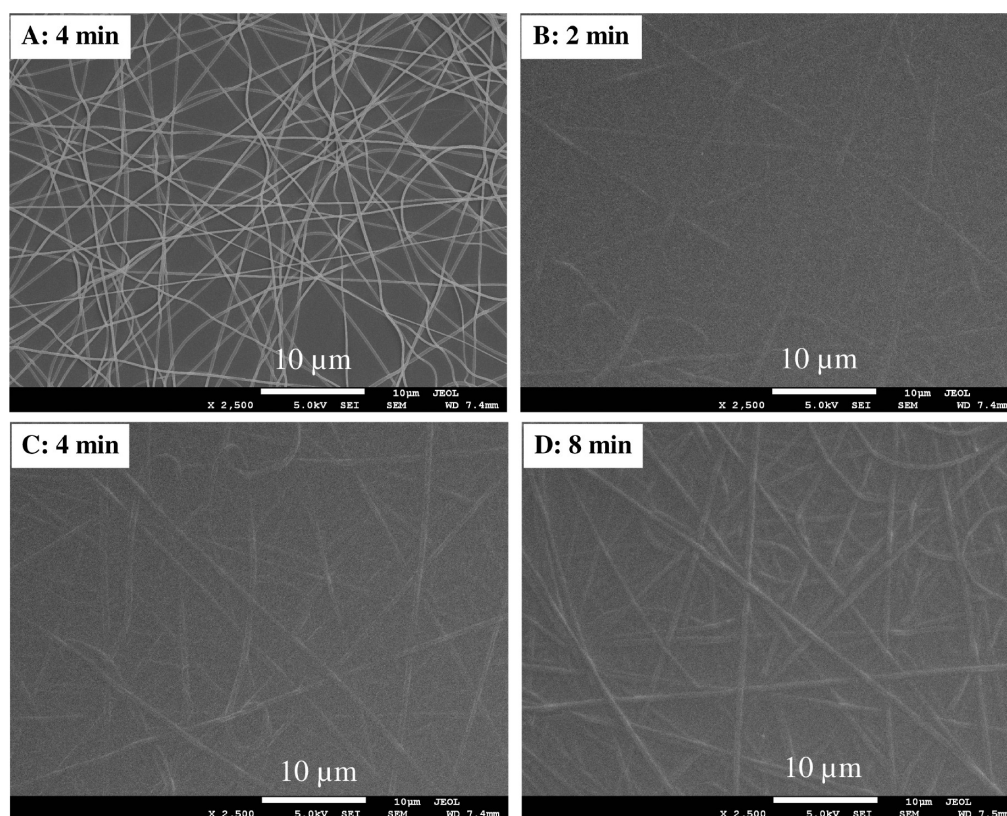


Figure 3. Surface morphologies of 2-layered TPU/nylon-6 nanofiber composite films (A: nylon-6 nanofibers on TPU film; B, C, and D: nylon-6 nanofibers embedded in TPU resin). The electrospinning time of A, B, C, and D were 4 min, 2 min, 4 min, and 8 min, respectively. Scale bar = 10 μm .

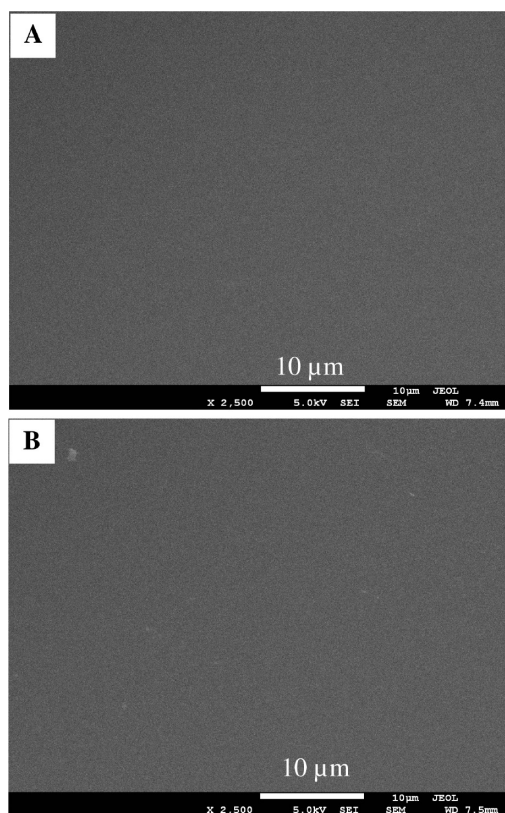


Figure 4. Surface morphologies of neat TPU film (A) and laminated TPU/nylon-6 nanofiber composite (B). Scale bar = 10 μm .

toughness. The toughness of composites is a measure of work done per unit mass to break the sample. It was determined by dividing the area under stress–strain curves with the density of the composites in a similar way as reported in the literature for other systems.³³ There was a significant increase in toughness of composite films (108 J/g for TPU; 274 J/g for reinforced TPU with 1.7 wt % of reinforcing fibers), and highly flexible films were obtained.

Generally, several factors will influence the mechanical properties of fiber reinforced composites: the original mechanical properties of the fibers, the dispersion of fibers in matrix, and the fiber/matrix interfacial interaction. In the present work, nylon-6 nanofibers were chosen as reinforcing fibers as they are already proved to be excellent reinforcing material in previous reports.^{21,23–25} The layer-by-layer (LBL) process used for making composites provided homogeneous dispersion of randomly deposited nylon-6 nanofibers in the TPU/DMF solution, as evidenced by the SEM images in Figure 3B,C,D. Also, due to the quick wetting process of nylon-6 nanofibers by DMF, as described before, the nylon-6 nanofibers were completely impregnated in the TPU matrix. This resulted in a strong interfacial morphology with no obvious edges between nanofibers and TPU matrix. The nanofibers were entirely embedded into the TPU matrix with no voids around the fibers as evidenced by the cross-section morphologies of the composites (Figure 7B,C,D). Additionally, the intermolecular interaction between nylon-6 and TPU, such as the hydrogen bonding as proved by FT-IR, could also be responsible for a strong interface. Therefore, during the tensile test, the load could be effectively transferred from the nylon-6 nanofibers to the TPU matrix, which resulted in the significant improvement

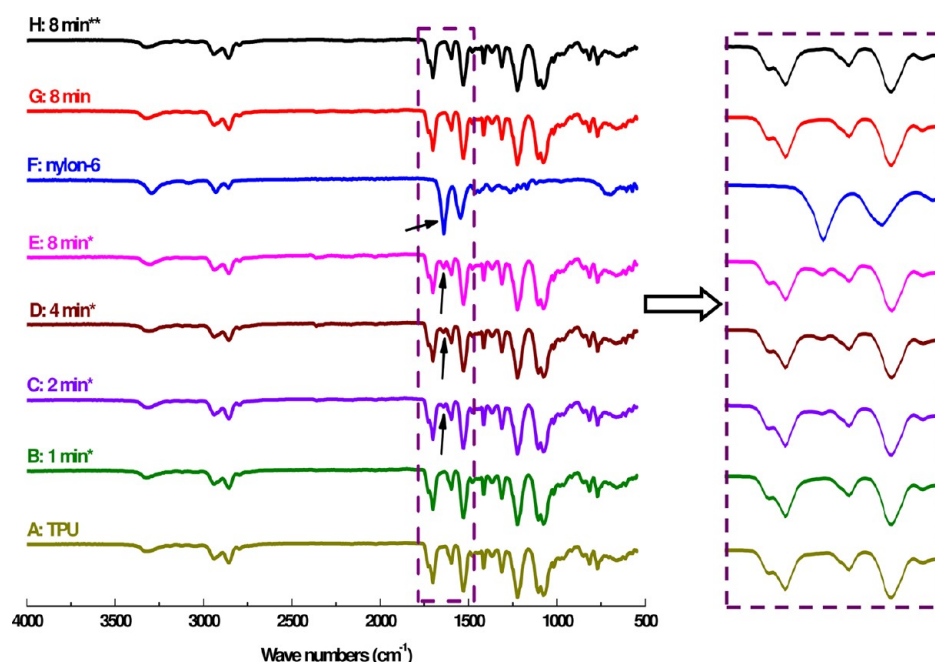


Figure 5. ATR-IR spectra of pure TPU film (A), neat PA-6 nanofiber mat (F), 2 layered TPU/nylon-6 nanofiber composite (B, C, D, E, and G), and laminated composite with 3 layers of nylon-6 nanofibers and 4 layers of TPU films (H).

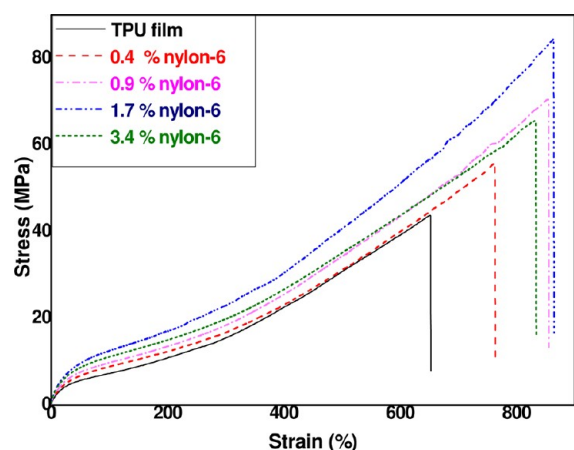


Figure 6. Typical stress–strain curves of TPU/nylon-6 nanofiber composite films with different amounts of reinforcing nylon-6 nanofibers.

of mechanical properties of the composites even with very small amount of nylon fibers. The small amounts of nylon fibers (0.4 wt %) already showed reinforcing effects although the optimum properties were achieved at 1.7 wt % of the reinforcing nylon fibers.

Figure 6 and Table 1 revealed that the electrospinning time (or the amount of nylon-6 nanofibers) had a significant effect

on the mechanical properties of the TPU/nylon-6 nanofiber composite films. On increasing the electrospinning time, the mechanical properties, including tensile strength, elongation at break, and E modulus first increased until about 4 min of electrospinning time (each layer was electrospun for 4 min and corresponded to about 1.7 wt % of nylon fibers) and then decreased on increasing the electrospinning time to 8 min.

To reveal the reasons for the mechanical properties trend, cross-section morphology of the composite films was investigated. This helped in commenting about the fiber distribution, the fiber amount in matrix, and the interaction between nanofibers and matrix. In order to obtain the original morphology without damage by the external forces, all the samples were first frozen in liquid nitrogen and then broken. As shown in Figure 7A,B,C,D, the neat TPU film presented a smooth cross-section while the composites revealed a rougher laminated morphology where 3 layers of nylon-6 nanofibers (white dots) were distributed in the TPU matrix (gray area). On increasing the electrospinning time from 2 to 4 min, there was an increase in the amount of homogeneously distributed load bearing reinforcing nanofibers in TPU matrix but importantly without any aggregation. When the electrospinning time was further increased to 8 min, there was an increase in the amount of nanofibers (Figure 7D) but they aggregated (Figure 7D, a) and formed defects, such as pulled-out nanofibers (Figure 7D, b), and holes/voids around the

Table 1. Summary of Mechanical Properties of the Neat TPU Film and TPU/Nylon-6 Nanofiber Composite Films with Varied Electrospinning Time (Nylon-6 Content) for Each Nanofiber Layer

nylon-6 content (%)	stress (MPa)	strain (%)	E modulus (2%) (MPa)	integration of stress–strain curves (MJ/m ³)	toughness (J/g)
0	42.27 ± 2.36	672.9 ± 40.3	27.1 ± 1.5	131.25 ± 11.21	108.47 ± 9.27
0.4	53.70 ± 3.67	753.4 ± 59.4	34.2 ± 1.9	183.92 ± 23.19	152.04 ± 19.17
0.9	64.82 ± 4.12	867.7 ± 52.6	35.9 ± 3.4	254.40 ± 22.95	210.39 ± 18.98
1.7	82.98 ± 6.19	876.0 ± 72.5	51.9 ± 6.7	332.14 ± 48.32	274.83 ± 39.98
3.4	60.32 ± 5.93	812.3 ± 70.5	49.0 ± 2.8	233.91 ± 38.85	193.78 ± 32.18

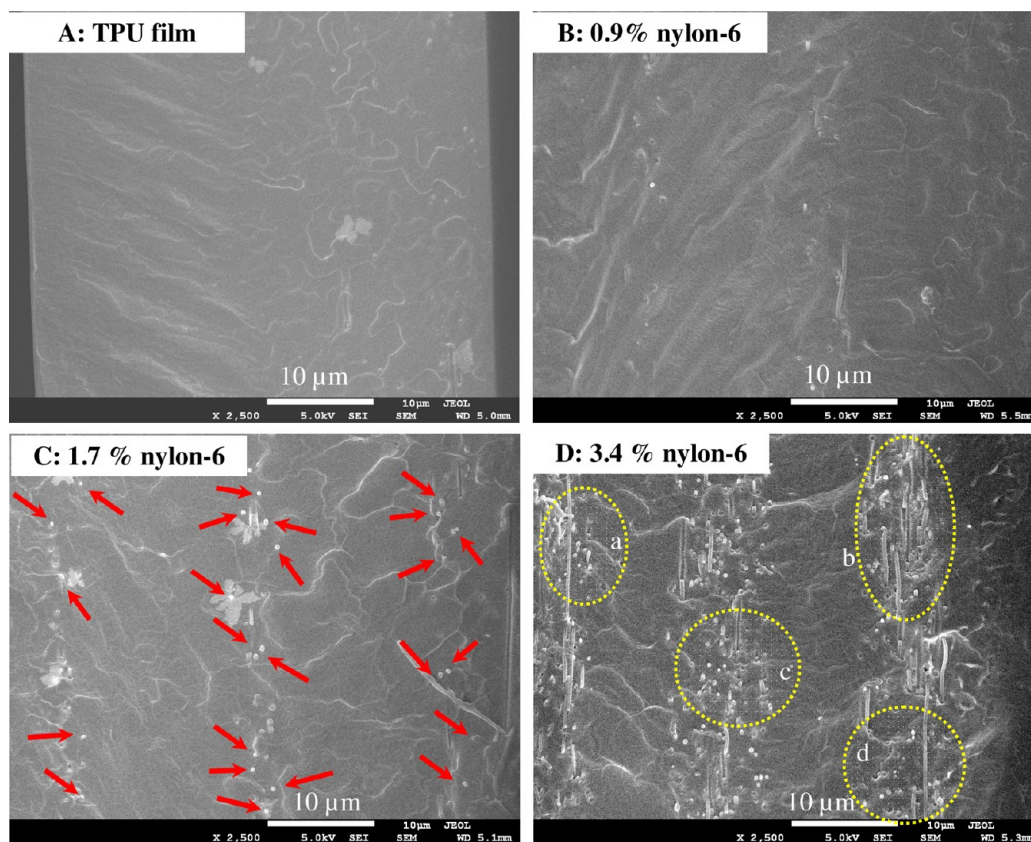


Figure 7. Cross-section morphologies of neat TPU film and laminated TPU/nylon-6 composites with varied electrospinning time on each layer. Scale bar = 10 μm .

nanofibers (Figure 7D, c and d). This led to reduction in mechanical properties.

The neat TPU film was transparent with light transmittance of 96% in the visible light range. In contrast, the nylon-6 nanofiber mat is opaque with no visible light transmittance (Figure 8). The nylon-6 nanofibers reinforced TPU composite films showed very high light transmittance and were transparent. The high transmittance of composite films might be the result of the small diameter of nylon-6 nanofibers and nearly

the same refractive index of the nylon-6 (1.53) and TPU (1.51).^{34,35} Although, the transmittance of the composites was dependent upon the amount of nylon fibers, but all composite films showed more than 85% light transmittance. The composite film with about 1.7 wt % of the reinforcing nylon-6 nanofibers showed the highest improvement in mechanical properties with very high (89%) light transmittance.

4. CONCLUSION

A novel procedure of making nanofiber reinforced thermoplastic films is successfully shown by taking nylon-6 nanofibers and thermoplastic polyurethane (TPU) as an example. The procedure is simple and can be extended to other thermoplastics. The significant reinforcement in mechanical properties of TPU like tensile strength, E modulus, elongation at break, and toughness could be seen just using very small amounts of nylon fibers. Even as small as 0.4 wt % of nylon fibers could improve mechanical properties significantly and increase further with an increase in the amount of fibers until an optimum amount was reached (1.7 wt % in this case). The mechanical properties were almost doubled at this amount. The enhanced mechanical properties were achieved without sacrificing optical properties like transparency of TPU.

■ AUTHOR INFORMATION

Corresponding Author

*Tel.: + (49) 6421 2825755. Fax: + (49) 6421 2825785. E-mail: agarwal@staff.uni-marburg.de.

Notes

The authors declare no competing financial interest.

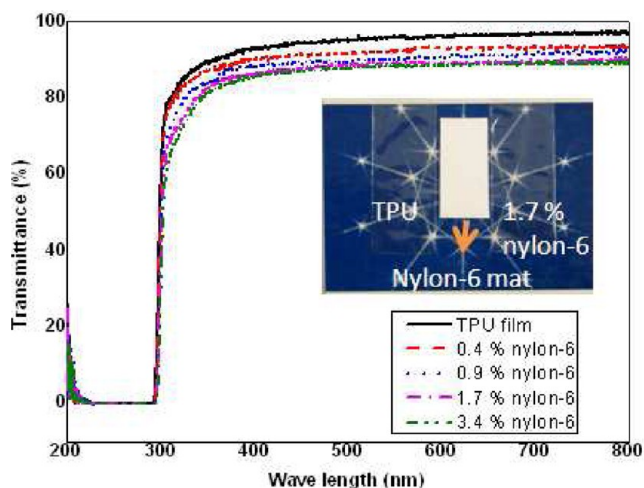


Figure 8. UV-vis spectra of TPU/nylon-6 nanofiber composite films (A) and digital photograph of transparent neat TPU film, nylon-6 nanofiber mat, and composite film (B).

■ REFERENCES

- (1) Hepburn, C. *Polyurethane elastomers*; Applied Science Publishers: Barking (Essex), 1982.
- (2) Oertel, G.; Abele, L. *Polyurethane handbook*; Hanser: München, Germany, 1993.
- (3) Walkor, B.; Rader, C. *Handbook of thermoplastic elastomer*; Van Nostrand Reinhold, New York, 1988.
- (4) Johnson, L.; Samms, J. *J. Ind. Text.* **1997**, *27*, 48–62.
- (5) Gao, C.; Abeysekera, J.; Hirvonen, M.; Aschan, C. *Int. J. Ind. Ergon.* **2003**, *31*, 323–330.
- (6) Tatai, L.; Moore, T. G.; Adhikari, R.; Malherbe, F.; Jayasekara, R.; Griffiths, I.; Gunatillake, P. A. *Biomaterials* **2007**, *28*, 5407–5417.
- (7) Özgür Seydibeyoğlu, M.; Oksman, K. *Compos. Sci. Technol.* **2008**, *68*, 908–914.
- (8) Pattanayak, A.; Jana, S. C. *Polym. Eng. Sci.* **2005**, *45*, 1532–1539.
- (9) Chen, Y.; Zhou, S.; Yang, H.; Gu, G.; Wu, L. *J. Colloid Interface Sci.* **2004**, *279*, 370–378.
- (10) Kutty, S. K. N.; Nando, G. B. *J. Appl. Polym. Sci.* **1991**, *43*, 1913–1923.
- (11) Corrêa, R. A.; Nunes, R. C. R.; Filho, W. Z. F. *Polym. Compos.* **1998**, *19*, 152–155.
- (12) Barick, A. K.; Tripathy, D. K. *Compos. Part A: Appl. Sci. Manuf.* **2010**, *41*, 1471–1482.
- (13) Greiner, A.; Wendorff, J. H. *Angew. Chem.* **2007**, *46* (30), 5670–5703.
- (14) Bergshoef, M. M.; Vancso, G. J. *Adv. Mater.* **1999**, *11*, 1362–1365.
- (15) Yano, H.; Sugiyama, J.; Nakagaito, A. N.; Nogi, M.; Matsuura, T.; Hikita, M.; Handa, K. *Adv. Mater.* **2005**, *17*, 153–155.
- (16) Liao, H.; Wu, Y.; Wu, M.; Zhan, X.; Liu, H. *Cellulose* **2012**, *19*, 111–119.
- (17) Zucchelli, A.; Focarete, M. L.; Gualandi, C.; Ramakrishna, S. *Polym. Adv. Technol.* **2011**, *22*, 339–349.
- (18) Kim, J.-S.; Reneker, D. H. *Polym. Compos.* **1999**, *20*, 124–131.
- (19) Stachewicz, U.; Peker, I.; Tu, W.; Barber, A. H. *ACS Appl. Mater. Interfaces* **2011**, *3*, 1991–1996.
- (20) Hang, F.; Lu, D.; J. Bailey, R.; Jimenez-Palomar, I.; Stachewicz, U.; Cortes-Ballesteros, B.; Davies, M.; Zech, M.; Bödefeld, C.; H. Barber, A. *Nanotechnology* **2011**, *22*, 365708.
- (21) Chen, L.-S.; Huang, Z.-M.; Dong, G.-H.; He, C.-L.; Liu, L.; Hu, Y.-Y.; Li, Y. *Polym. Compos.* **2009**, *30*, 239–247.
- (22) Romo-Urbe, A.; Arizmendi, L.; Romero-Guzmán, M. a. E.; Sepúlveda-Guzmán, S.; Cruz-Silva, R. *ACS Appl. Mater. Interfaces* **2009**, *1*, 2502–2508.
- (23) Neppalli, R.; Marega, C.; Marigo, A.; Bajgai, M. P.; Kim, H. Y.; Causin, V. *Polymer* **2011**, *52*, 4054–4060.
- (24) Fong, H. *Polymer* **2004**, *45*, 2427–2432.
- (25) Tian, M.; Gao, Y.; Liu, Y.; Liao, Y.; Xu, R.; Hedin, N. E.; Fong, H. *Polymer* **2007**, *48*, 2720–2728.
- (26) Tang, C.; Liu, H. *Compos. Part A: Appl. Sci. Manuf.* **2008**, *39*, 1638–1643.
- (27) Mollá, S.; Compañ, V. J. *Membr. Sci.* **2011**, *372*, 191–200.
- (28) Lin, S.; Cai, Q.; Ji, J.; Sui, G.; Yu, Y.; Yang, X.; Ma, Q.; Wei, Y.; Deng, X. *Compos. Sci. Technol.* **2008**, *68*, 3322–3329.
- (29) Wu, M.; Wu, Y.; Liu, Z.; Liu, H. *J. Compos. Mater.* **2012**.
- (30) Chen, Y.; Han, D.; Ouyang, W.; Chen, S.; Hou, H.; Zhao, Y.; Fong, H. *Compos. Part B: Eng.* **2012**, *43*, 2382–2388.
- (31) Akangah, P.; Lingaiah, S.; Shivakumar, K. *Compos. Struct.* **2010**, *92*, 1432–1439.
- (32) Jiang, S.; Hou, H.; Greiner, A.; Agarwal, S. *ACS Appl. Mater. Interfaces* **2012**, *4* (5), 2597–2603.
- (33) Blond, D.; Barron, V.; Ruether, M.; Ryan, K. P.; Nicolosi, V.; Blau, W. J.; Coleman, J. N. *Adv. Funct. Mater.* **2006**, *16*, 1608–1614.
- (34) Gaur, H. A.; De Vries, H. J. *Polym. Sci. Polym. Phys. Ed.* **1975**, *13*, 835–850.
- (35) Wu, J.-H.; Li, C.-H.; Wu, Y.-T.; Leu, M.-T.; Tsai, Y. *Compos. Sci. Technol.* **2010**, *70*, 1258–1264.